Strange axial and vector form factors of the nucleon from lattice QCD

Jeremy Green

Institut für Kernphysik, Johannes Gutenberg-Universität Mainz

Hadronic Contributions to New Physics Searches
September 25–30, 2016

Outline

1. Introduction
2. Lattice QCD
3. Strange electromagnetic form factors
4. Light and strange axial form factors
5. Summary

Nucleons

The *net* quark content of a proton is *uud* and of a neutron is *ddu*.

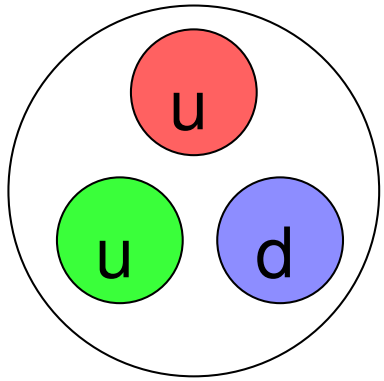

But quantum fluctuations can produce gluons and $\bar{q}q$ pairs, including also heavier quarks (s, ...).

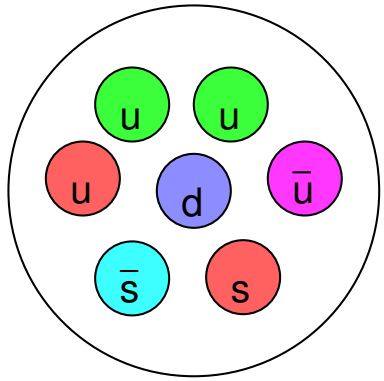

Nucleon vector and axial form factors

Describe the strength of the coupling of a proton to a current:

$$\langle p'|V_\mu^q|p\rangle = \bar{u}(p')\left[\gamma_\mu F_1^q(Q^2) + \frac{i\sigma_{\mu\nu}(p'-p)^\nu}{2m_p}F_2^q(Q^2)\right]u(p)$$

$$\langle p'|A_\mu^q|p\rangle = \bar{u}(p')\left[\gamma_\mu G_A^q(Q^2) + \frac{(p'-p)_\mu}{2m_p}G_P^q(Q^2)\right]\gamma_5 u(p),$$

where $V_\mu^q = \bar{q}\gamma_\mu q$ and $A_\mu^q = \bar{q}\gamma_\mu\gamma_5 q$.
Electric and magnetic form factors:

$$G_E^q(Q^2) = F_1^q(Q^2) - \frac{Q^2}{(2m_p)^2}F_2^q(Q^2), \quad G_M^q(Q^2) = F_1^q(Q^2) + F_2^q(Q^2).$$

Elastic *ep* scattering

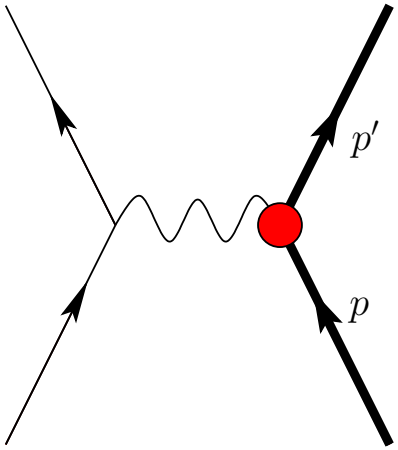

Elastic scattering of an electron off a fixed proton target has a leading contribution from single photon exchange, which is sensitive to

$$G_{E,M}^{\gamma(p)} = \tfrac{2}{3} G_{E,M}^{u} - \tfrac{1}{3} G_{E,M}^{d} - \tfrac{1}{3} G_{E,M}^{s} + \ldots$$

The contribution to the cross section is

$$\sigma \propto G_E^{\gamma(p)}(Q^2)^2 + \frac{\tau}{\epsilon} G_M^{\gamma(p)}(Q^2)^2, \qquad \tau = \frac{Q^2}{4m_p^2}, \quad \epsilon^{-1} = 1 + 2(2+\tau)\tan^2\tfrac{\theta}{2},$$

thus allowing the form factors to be measured in experiments.

Electromagnetic form factors

In the *nonrelativistic limit*, $G_E(Q^2)$ and $G_M(Q^2)$ are Fourier transforms of the charge and magnetization densities in a proton.

- $G_E^\gamma(0) = 1$, the charge of a proton
- $G_M^\gamma(0) = \mu$, the magnetic moment of a proton, in units of the nuclear magneton $\mu_N = \frac{e}{2m_p}$

Even though this interpretation doesn't hold relativistically, it is still used to *define* the charge and magnetic radii using the derivatives at $Q^2 = 0$:

- $r_E^2 = -6G_E^{\gamma\,\prime}(0)$
- $r_M^2 = -6G_M^{\gamma\,\prime}(0)/\mu$

Relativistically, there is a rigorous interpretation of $F_1(Q^2)$ as the 2-D Fourier transform of the transverse charge density in the infinite-momentum frame.

Aside: radius from spectroscopy

Spectroscopy is also sensitive to the proton r_E.

In a hydrogen atom, the S orbitals have the proton located at an antinode of the electron's wavefunction, whereas the P orbitals have it located at a node.

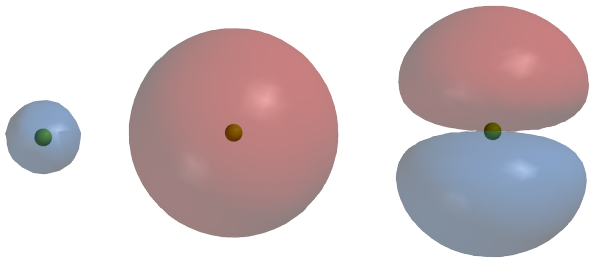

Thus the 2S–2P Lamb shift is sensitive to the finite radius of the proton.

If the electron is replaced by a muon (200× heavier), the orbitals will be smaller and the effect becomes bigger (2% of the Lamb shift).

Aside: proton radius problem

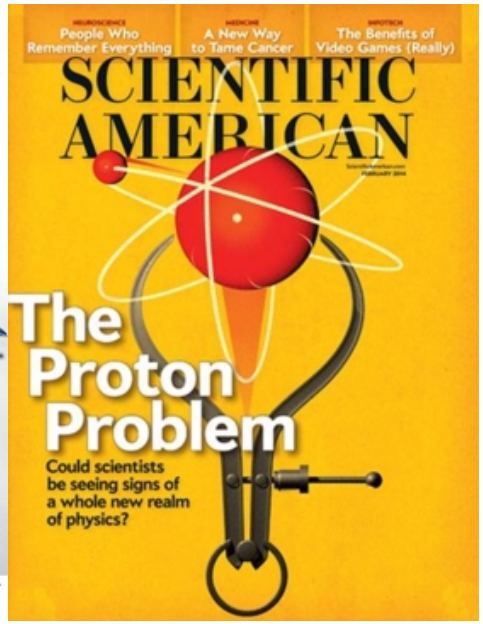

7σ discrepancy between results from Lamb shift and muonic hydrogen and combined results from electron-proton scattering+spectroscopy.

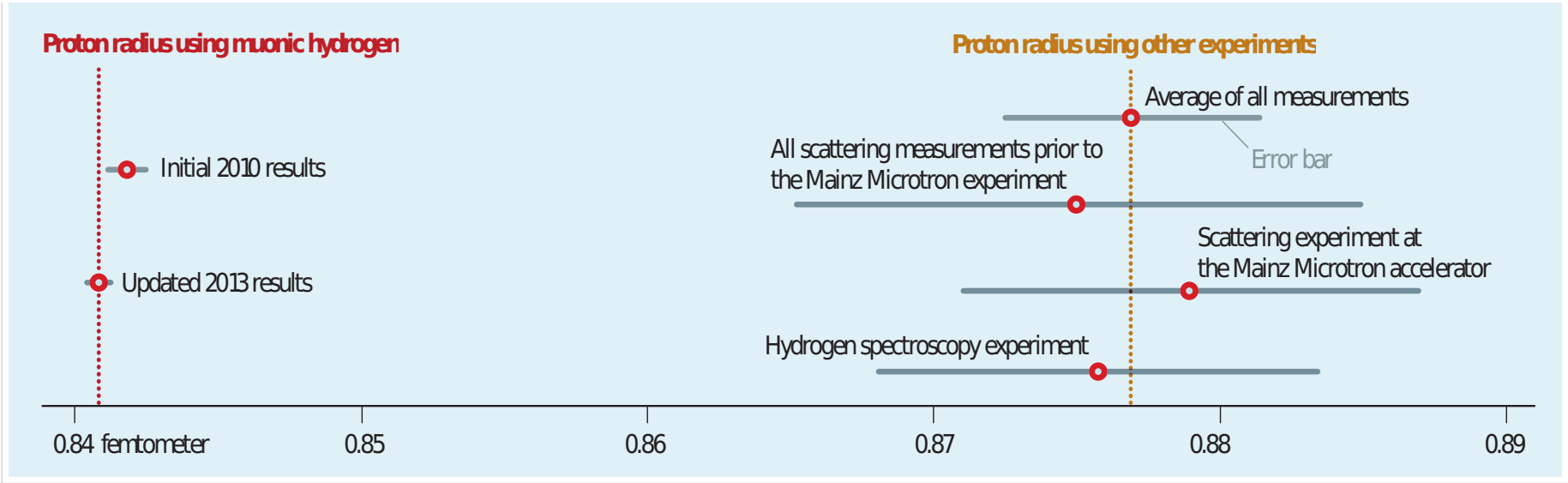

J. C. Bernauer and R. Pohl, Scientific American, February 2014

Measuring strange form factors

Using a single probe (photons) and two targets (protons and neutrons), assuming isospin allows for isolating two flavour contributions, u and d.

To isolate the next-largest contribution, from s quarks, use a different probe: Z bosons.

$$J_\mu^{ZV} = (1 - \tfrac{8}{3}\sin^2\theta_W)\,\bar{u}\gamma_\mu u - (1 - \tfrac{4}{3}\sin^2\theta_W)(\bar{d}\gamma_\mu d + \bar{s}\gamma_\mu s) + \ldots$$

By measuring the parity-violating asymmetry in elastic $\vec{e}p$ scattering,

$$A_{PV} = \frac{\sigma_R - \sigma_L}{\sigma_R + \sigma_L},$$

the leading single-photon-exchange contribution can be eliminated and the interference between γ and Z exchange diagrams can be isolated.

Experiments at forward scattering angles

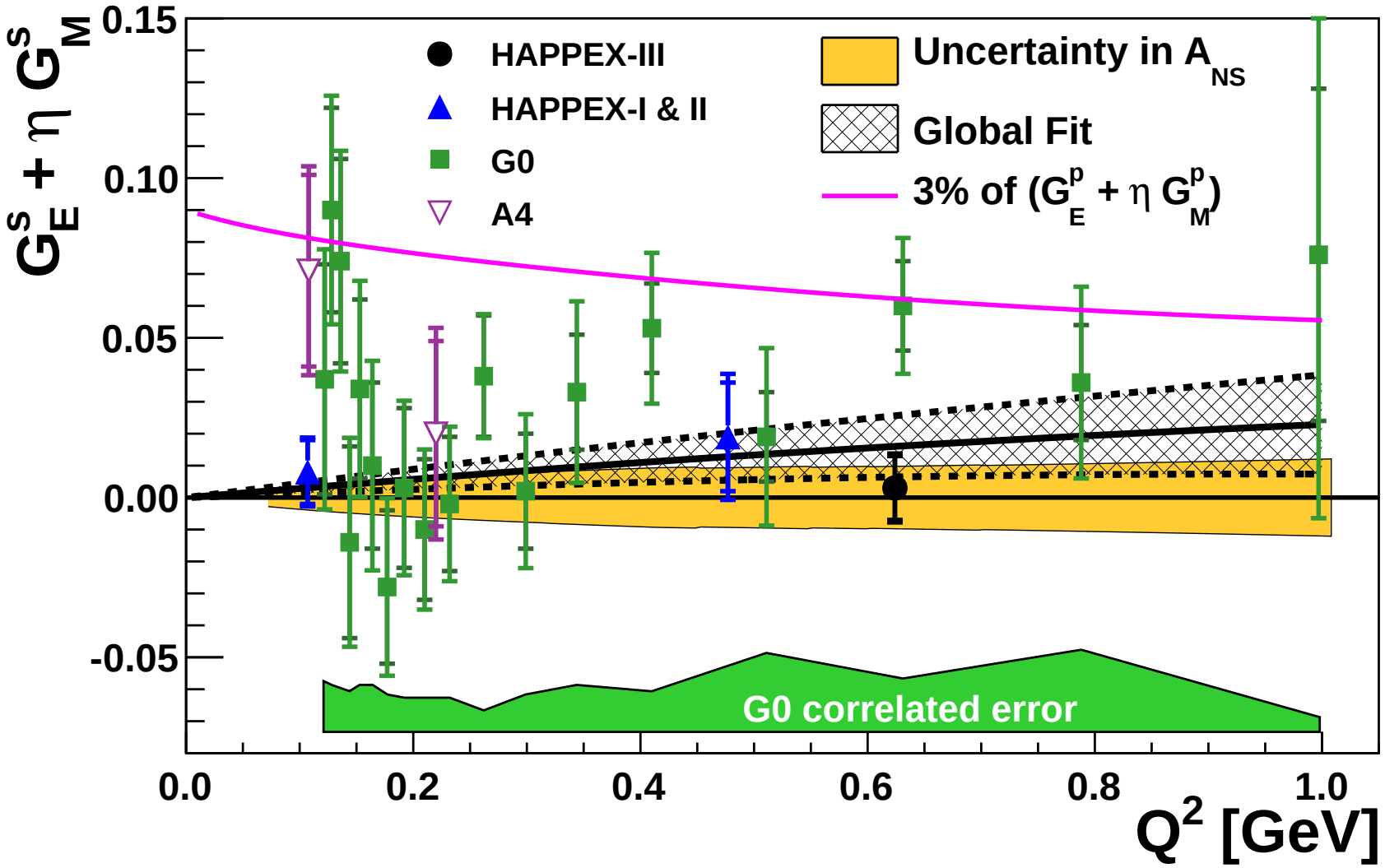

$\eta \approx AQ^2$, $A = 0.94\ \text{GeV}^{-2}$

HAPPEX Collaboration, Phys. Rev. Lett. **108** (2012) 102001 [1107.0913]

G_E^s and G_M^s at $Q^2 \approx 0.62$ GeV^2

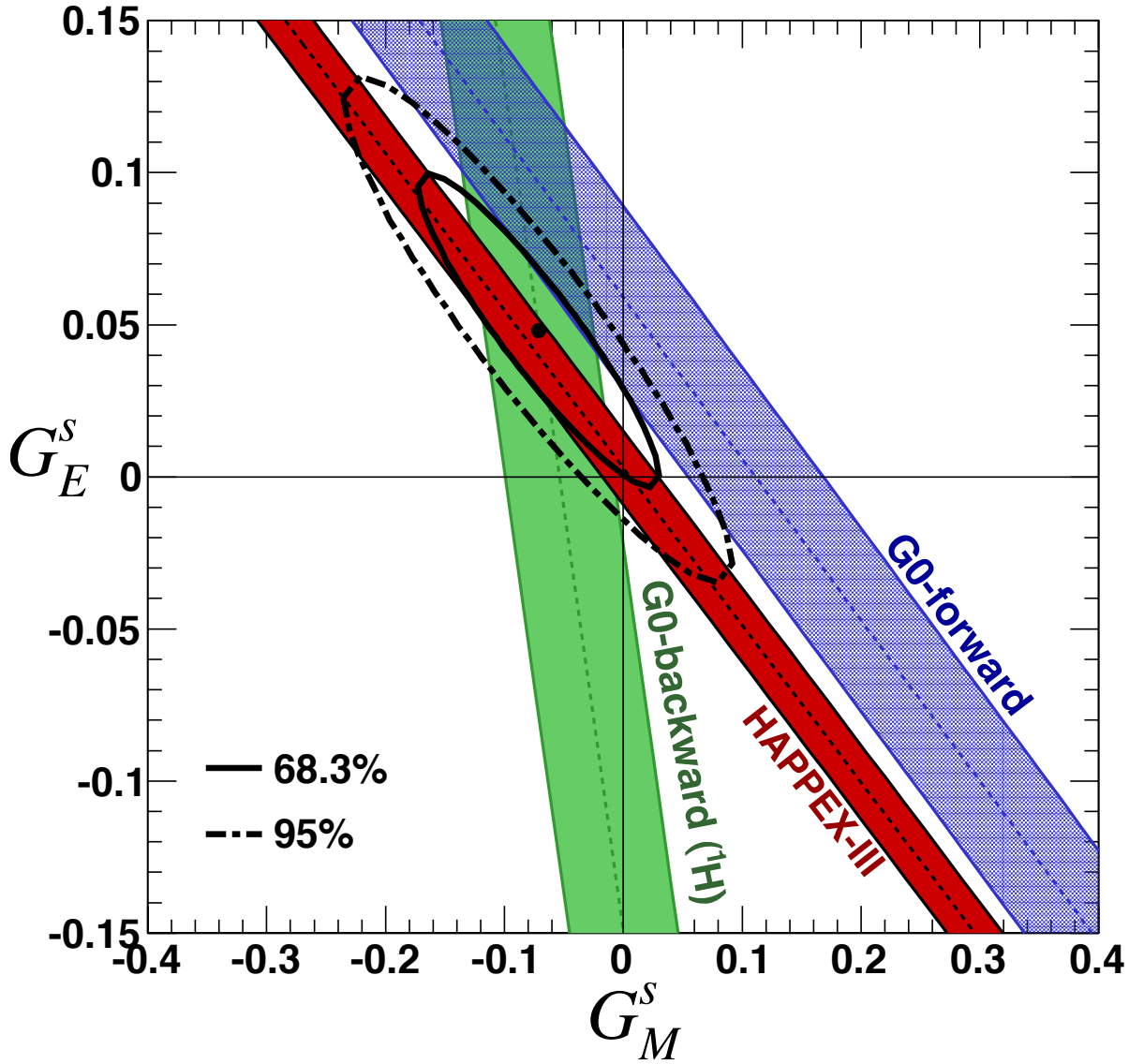

HAPPEX Collaboration, Phys. Rev. Lett. **108** (2012) 102001 [1107.0913]

Axial form factors

Assuming isospin, the interaction between nucleons and a W boson contains the isovector axial current A_μ^{u-d}.

- Axial charge $g_A^{u-d} \equiv G_A^{u-d}(0) = 1.2723(23)$ measured from neutron beta decay. This has long served as a "benchmark" for lattice QCD.
- Quasielastic neutrino scattering, e.g. $\nu_e n \to e^- p$, is sensitive to G_A^{u-d}.
- Muon capture, $\mu^- p \to \nu_\mu n$, is sensitive to G_P^{u-d}.

The interaction between a proton and a Z boson contains the axial current A_μ^{u-d-s}.

- Relevant for elastic νp and parity-violating elastic ep scattering.

Quark spin in the proton

$g_A^q \equiv G_A^q(0)$ gives the contribution from the spin of q to the proton's spin.
This equals the moment of a polarized parton distribution function:

$$g_A^q = \int_0^1 dx \left(\Delta q(x) + \Delta \bar{q}(x)\right) .$$

For the typical phenomenological values:

- g_A^{u-d} is obtained from neutron beta decay.
- g_A^{u+d-2s} is obtained from semileptonic beta decay of octet baryons, assuming $SU(3)$ symmetry.
- A third linear combination is obtained from the integral of polarized PDFs measured in polarized deep inelastic scattering.

Important for spin-dependent dark matter scattering.

Lattice QCD

...is a regularization of Euclidean-space QCD such that the path integral can be done fully non-perturbatively

- Euclidean spacetime becomes a periodic hypercubic lattice, with spacing a and box size $L_s^3 \times L_t$.
- Path integral over fermion degrees of freedom is done analytically, for each gauge configuration. Solving the Dirac equation with a fixed source yields a source-to-all quark propagator.
- Path integral over gauge degrees of freedom is done numerically using Monte Carlo methods to generate an *ensemble* of *gauge configurations*.

The $a \to 0$ and $L_s, L_t \to \infty$ extrapolations need to be taken by using multiple ensembles.

Nucleon matrix elements using lattice QCD

To find matrix elements, compute using an interpolating operator χ:

$$C_{2\mathrm{pt}}(t,\vec{p}) = \sum_{\vec{x}} e^{-i\vec{p}\cdot\vec{x}} \langle \chi(\vec{x},t)\bar{\chi}(\vec{0},0)\rangle$$

$$\xrightarrow{t\to\infty} e^{-E(\vec{p})t} |\langle p|\bar{\chi}|\Omega\rangle|^2$$

$$C_{3\mathrm{pt}}(T,\tau;\vec{p},\vec{p}\,') = \sum_{\vec{x},\vec{y}} e^{-i\vec{p}\,'\cdot\vec{x}} e^{i(\vec{p}\,'-\vec{p})\cdot\vec{y}} \langle \chi(\vec{x},T)\mathcal{O}(\vec{y},\tau)\bar{\chi}(\vec{0},0)\rangle$$

$$\xrightarrow[T-\tau\to\infty]{\tau\to\infty} e^{-E(\vec{p}\,')(T-\tau)} e^{-E(\vec{p})\tau} \langle\Omega|\chi|p'\rangle\langle p'|\mathcal{O}|p\rangle\langle p|\bar{\chi}|\Omega\rangle$$

Then form ratios to isolate $\langle p'|\mathcal{O}|p\rangle$.
For $\mathcal{O}$ a quark bilinear, there are two kinds of quark contractions for $C_{3\mathrm{pt}}$:

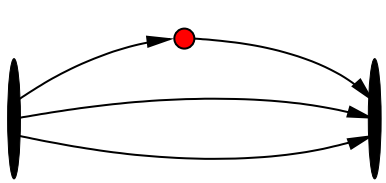

connected

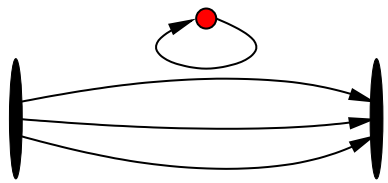

disconnected

Connected contractions

We have efficient solvers for source-to-all quark propagators. Connected contractions can be computed using these via the *sequential propagator* technique.

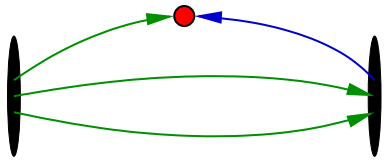

1. Fix the source and compute the forward propagator.
2. Fix the sink and T; compute the backward (sequential) propagator.
3. Combine the two to compute arbitrary $\mathcal{O} = \bar{q} \ldots q$, for all $\tau \in [0, T]$.

For the proton, these contribute for $q \in \{u, d\}$. If we take isovector $(u - d)$ observables, then these are the only contributing contractions.

Disconnected contractions

For strange quarks in the proton, these are the only contribution.
Disconneced light quarks are also needed for, e.g., the proton radius.

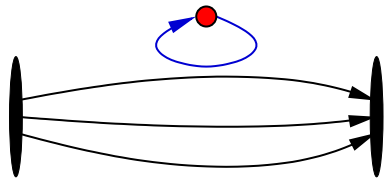

Using, e.g., $\mathcal{O} = \bar{q}\Gamma q$, these involve the disconnected loop,

$$T(\vec{q}, t, \Gamma) = -\sum_{\vec{x}} e^{i\vec{q}\cdot\vec{x}}\,\mathrm{Tr}[\Gamma D^{-1}(x,x)],$$

which involves the quark propagator $D^{-1}(x,y)$ from every point on a timeslice back to itself.
We can estimate the all-to-all propagator stochastically using noise sources η that satisfy $E(\eta\eta^\dagger) = I$. By solving $\psi = D^{-1}\eta$, we get

$$D^{-1}(x,y) = E(\psi(x)\eta^\dagger(y)).$$

Dilution

For a random vector η with components of magnitude $|\eta_i| = 1$, the diagonal of $\eta\eta^\dagger$ is exact and the variance comes from the off-diagonal parts.

$$\text{e.g.} \quad \eta = \begin{pmatrix} \eta_1 \\ \eta_2 \\ \eta_3 \\ \eta_4 \end{pmatrix}, \quad \eta\eta^\dagger = \begin{pmatrix} 1 & \eta_1\eta_2^* & \eta_1\eta_3^* & \eta_1\eta_4^* \\ \eta_2\eta_1^* & 1 & \eta_2\eta_3^* & \eta_2\eta_4^* \\ \eta_3\eta_1^* & \eta_3\eta_2^* & 1 & \eta_3\eta_4^* \\ \eta_4\eta_1^* & \eta_4\eta_2^* & \eta_4\eta_3^* & 1 \end{pmatrix}, \quad E(\eta\eta^\dagger) = I$$

Dilution: use a complete set of projectors $\{P_b | P_b^2 = P_b, \sum_b P_b = I\}$ to partition the components of η and eliminate parts of the variance:

$$\eta^{(b)} \equiv P_b\eta; \qquad E\left(\sum_b \eta^{(b)}\eta^{(b)\dagger}\right) = I$$

$$\text{e.g.} \quad \eta^{(1)} = \begin{pmatrix} \eta_1 \\ \eta_2 \\ 0 \\ 0 \end{pmatrix}, \eta^{(2)} = \begin{pmatrix} 0 \\ 0 \\ \eta_3 \\ \eta_4 \end{pmatrix}, \quad \sum_b \eta^{(b)}\eta^{(b)\dagger} = \begin{pmatrix} 1 & \eta_1\eta_2^* & 0 & 0 \\ \eta_2\eta_1^* & 1 & 0 & 0 \\ 0 & 0 & 1 & \eta_3\eta_4^* \\ 0 & 0 & \eta_4\eta_3^* & 1 \end{pmatrix}$$

Dilution

In many cases, using N dilution projectors to target the most important parts of the noise yields a better than $1/\sqrt{N}$ reduction. Commonly used:

- Spin dilution
- Colour dilution
- Spatial dilution

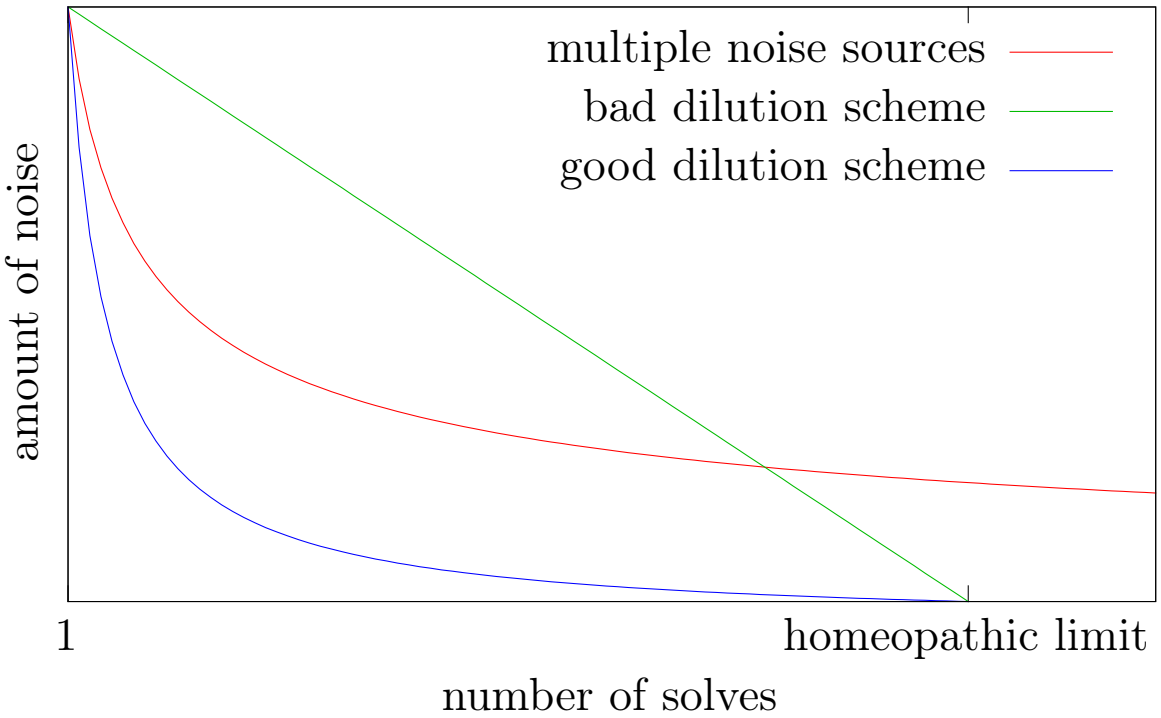

In the *homeopathic limit*, complete dilution is equivalent to fully computing a disconnected loop without stochastic estimation.

Hadamard vectors

Hadamard vectors h_b can be used to obtain the same results as dilution, by taking the component-wise product $\eta^{[b]} \equiv h_b \odot \eta$ and averaging over b.
e.g. Hadamard vectors: $h_1 = (1,1,1,1)$, $h_2 = (1,1,-1,-1)$

$$\eta^{[1]} = \begin{pmatrix} \eta_1 \\ \eta_2 \\ \eta_3 \\ \eta_4 \end{pmatrix}, \eta^{[2]} = \begin{pmatrix} \eta_1 \\ \eta_2 \\ -\eta_3 \\ -\eta_4 \end{pmatrix}, \quad \frac{1}{2}\sum_b \eta^{[b]}\eta^{[b]\dagger} = \begin{pmatrix} 1 & \eta_1\eta_2^* & 0 & 0 \\ \eta_2\eta_1^* & 1 & 0 & 0 \\ 0 & 0 & 1 & \eta_3\eta_4^* \\ 0 & 0 & \eta_4\eta_3^* & 1 \end{pmatrix}$$

If we had used only $\eta^{[1]}$, we would also get the correct expectation value (only with more noise).
$\longrightarrow$ Hadamard vectors allow for progressively increasing the level of dilution, while making use of previous effort.

Hierarchical probing

A. Stathopoulos, J. Laeuchli, K. Orginos, SIAM J. Sci. Comput. **35(5)** (2013) S299–S322 [1302.4018]

Use a sequence of specially-constructed spatial Hadamard vectors in order to progressively increase the level of spatial dilution.

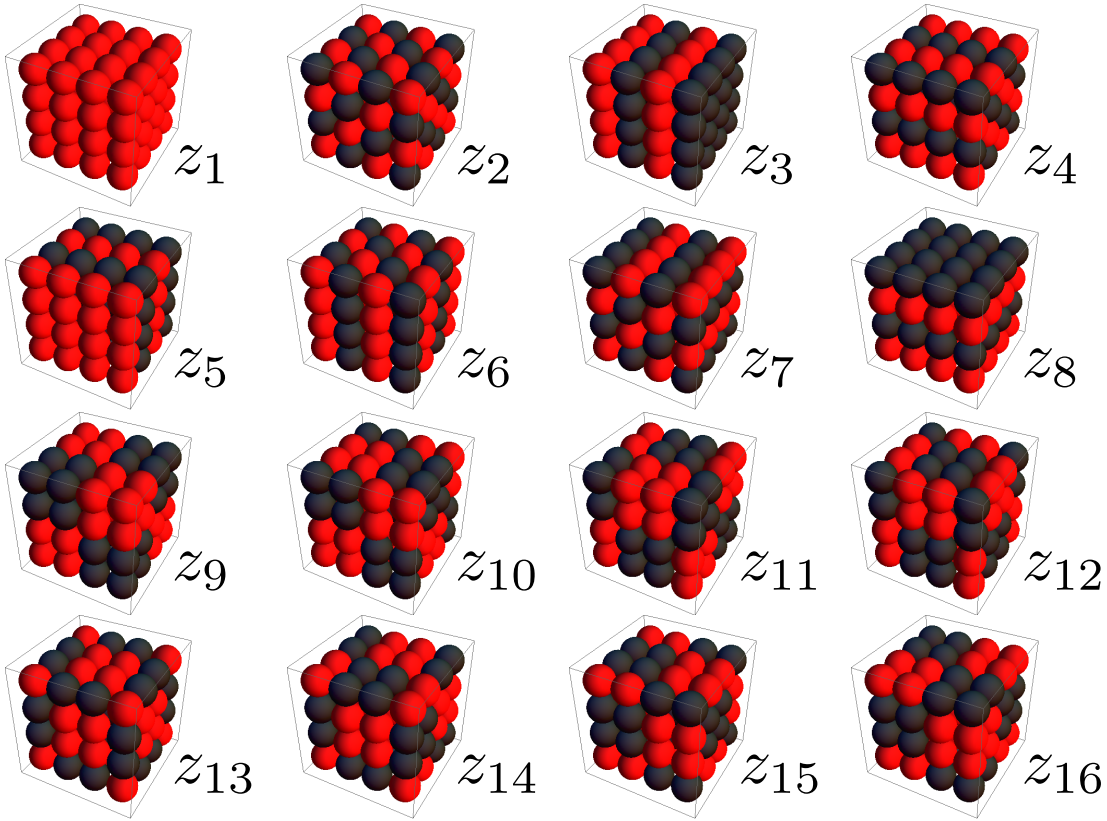

red: $+1$
black: -1

We use 128 three-dimensional Hadamard vectors to eliminate the variance from neighboring sites up to distance 7.

Fitting Q^2-dependence

We want to fit $G_{E,M,A,P}(Q^2)$ with curves to characterize the overall shape of the form factor, and determine the intercepts and/or radii.

- Common approach: use simple fit forms such as a dipole.
- Better: use z-expansion. Conformally map domain where $G(Q^2)$ is analytic in complex Q^2 to $|z| < 1$, then use a Taylor series:

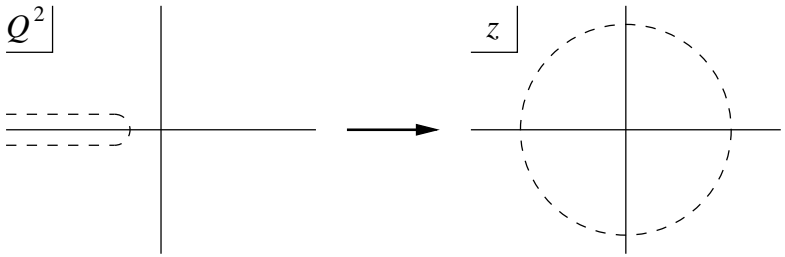

$$z(Q^2) = \frac{\sqrt{t_{\text{cut}} + Q^2} - \sqrt{t_{\text{cut}}}}{\sqrt{t_{\text{cut}} + Q^2} + \sqrt{t_{\text{cut}}}},$$

$$G(Q^2) = \sum_k a_k z(Q^2)^k,$$

e.g. R. J. Hill and G. Paz, Phys. Rev. D **84** (2011) 073006

with Gaussian priors imposed on the coefficients a_k.

- Leave a_0 and a_1 unconstrained, so that the intercept and slope are not directly constrained.
- For higher coefficients, impose $|a_{k>1}| < 5 \max\{|a_0|, |a_1|\}$, and vary the bound to estimate systematic uncertainty.

For G_P, perform the fit to $(Q^2 + m^2)G_P(Q^2)$ to remove the pseudoscalar pole.

Lattice calculation: strange electromagnetic form factors

JG, S. Meinel, M. Engelhardt, S. Krieg, J. Laeuchli, J. Negele, K. Orginos, A. Pochinsky, S. Syritsyn, Phys. Rev. D **92** (2015) 031501(R) [1505.01803]

- Ensemble generated by JLab / William & Mary
- $N_f = 2 + 1$ Wilson-clover fermions
- $a = 0.114$ fm, $32^3 \times 96$
- $m_u = m_d > m_{ud}^{\text{phys}}$, corresponding to pion mass 317 MeV
- $m_s \approx m_s^{\text{phys}}$
- 1028 gauge configurations
- disconnected loops for six source timeslices
  (128 Hadamard vectors, plus color+spin dilution)
- two-point correlators from 96 source positions

Hierarchical probing vs. many noise sources

Study using 1/3 of gauge configurations.

$G_M^{(\frac{2}{3}u-\frac{1}{3}d)}$ $(Q^2 \approx 0.11\ \mathrm{GeV}^2)$ (disconnected)

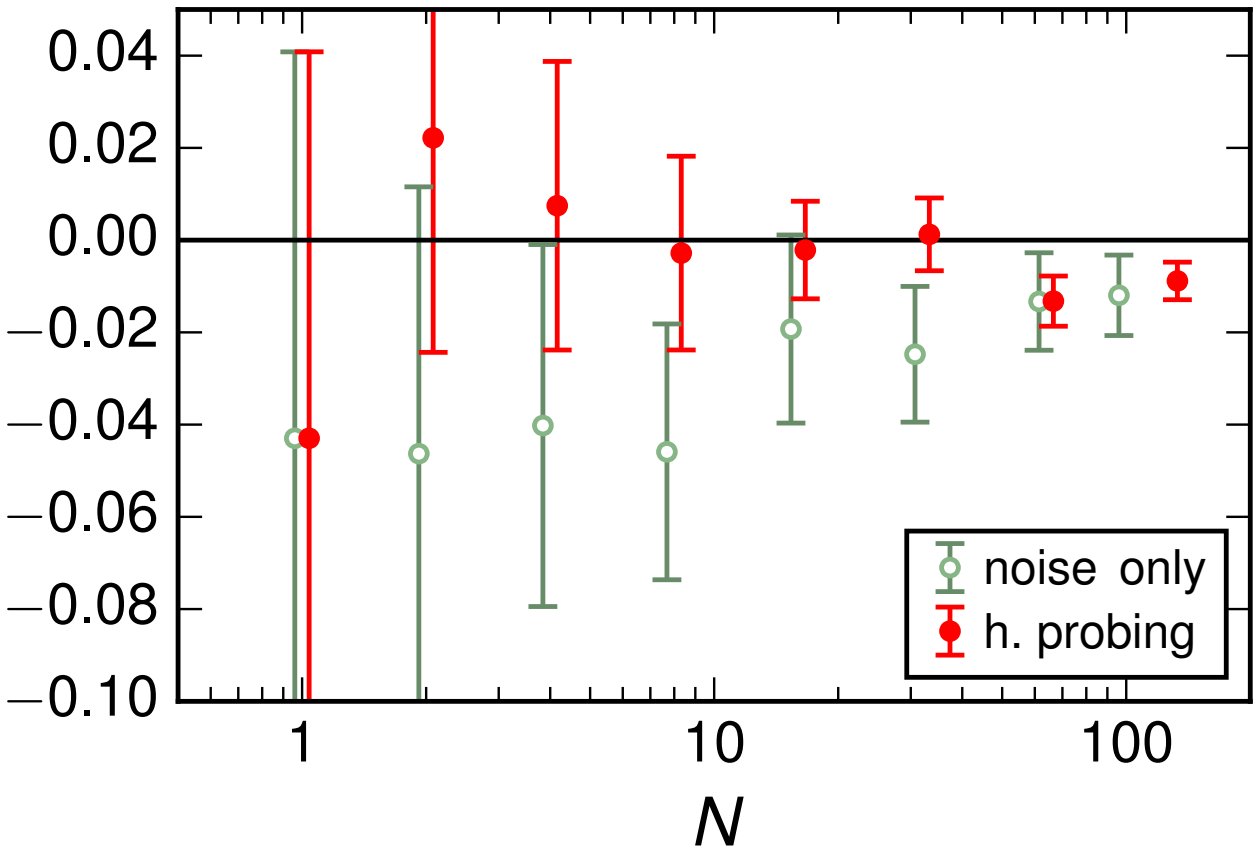

Equal cost at same N (= N_{Hadamard} or N_{noise}).

Points offset horizontally.

(S. Meinel, Lattice 2014)

Disconnected $G_E(Q^2)$

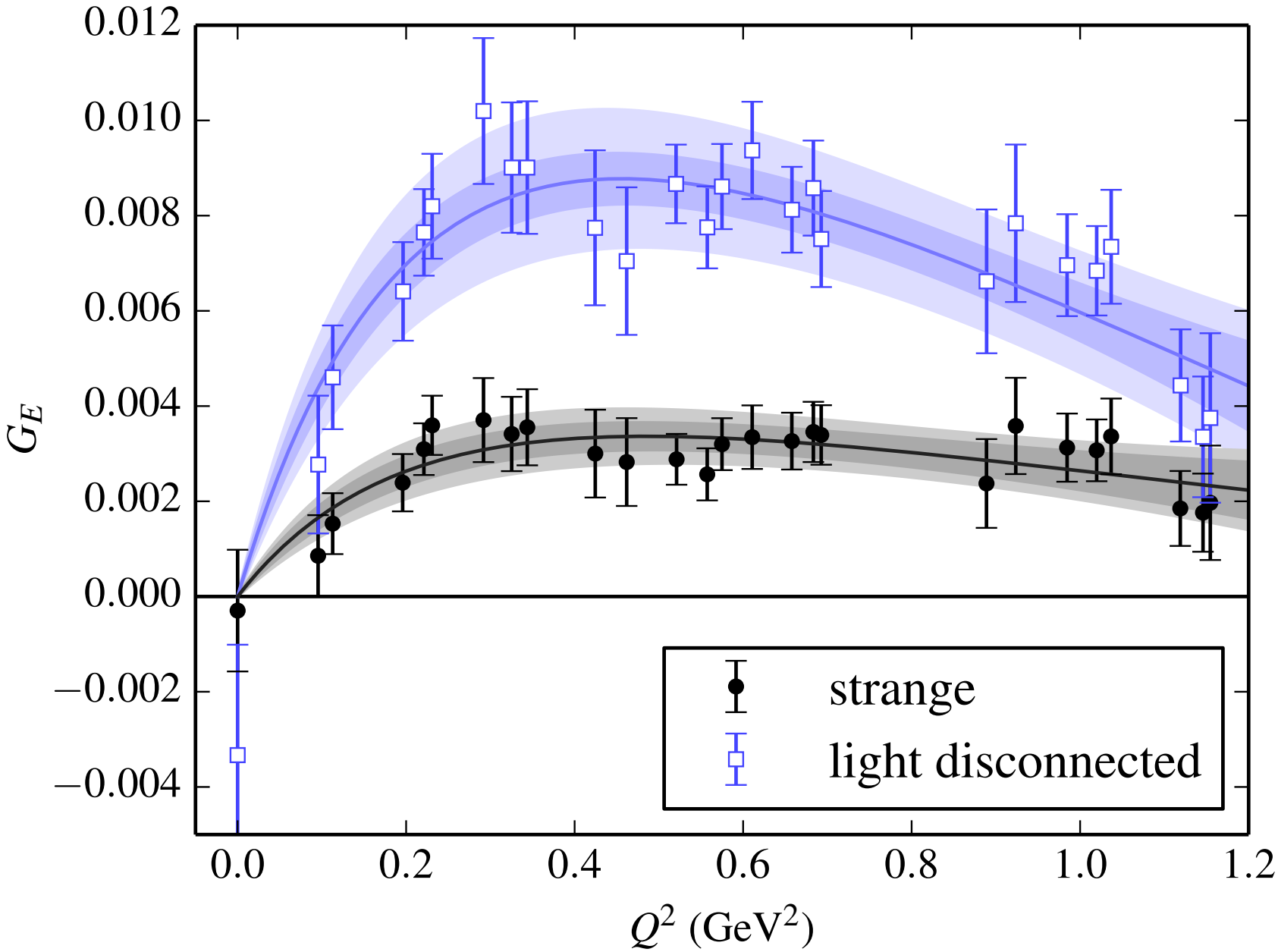

Disconnected $G_M(Q^2)$

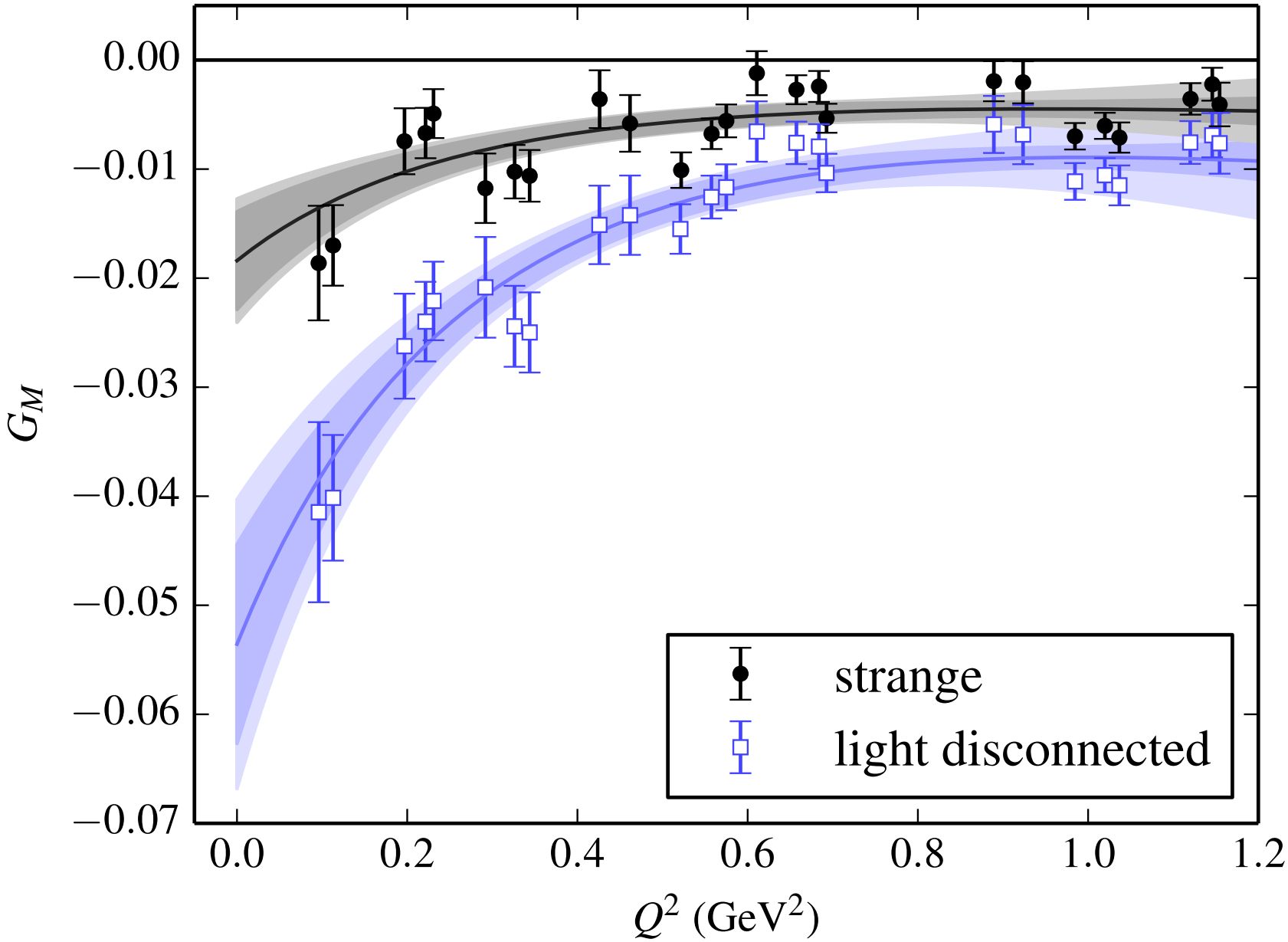

Strange magnetic moment and radii at $m_\pi = 317$ MeV

For the unphysical quark masses used on this ensemble:

$$\begin{aligned}(r_E^2)^s &= -0.0054(9)(6)(11)(2)\ \text{fm}^2,\\ (r_M^2)^s &= -0.0147(61)(28)(34)(5)\ \text{fm}^2,\\ \mu^s &= -0.0184(45)(12)(32)(1)\ \mu_N^{\text{lat}},\end{aligned}$$

where the uncertainties are

1. statistical
2. fitting
3. excited states
4. discretization

Finite-volume effects neglected since $m_\pi L = 5.9$.

Contributions to proton electromagnetic obervables

Use crude extrapolation to the physical pion mass inspired by partially-quenched ChPT. Compare strange observable X^s to proton electromagnetic observable X^p that can be written as

$$X^p = (u,\, d \text{ contributions}) - \frac{1}{3} X^s$$

X^s	X^p
$(r_E^2)^s = -0.0067(10)(17)(15)\ \text{fm}^2$	$(r_E^2)^p \approx (0.88\ \text{fm})^2$
$\mu^s = -0.022(4)(4)(6)\ \mu_N$	$\mu^p = 2.793\ \mu_N$
$(r_M^2)^s = -0.018(6)(5)(5)\ \text{fm}^2$	$\mu^p (r_M^2)^p \approx 2.793(0.85\ \text{fm})^2$

In all three cases, the strange-quark contribution is ~ 0.3–0.4%.

Strange magnetic moment

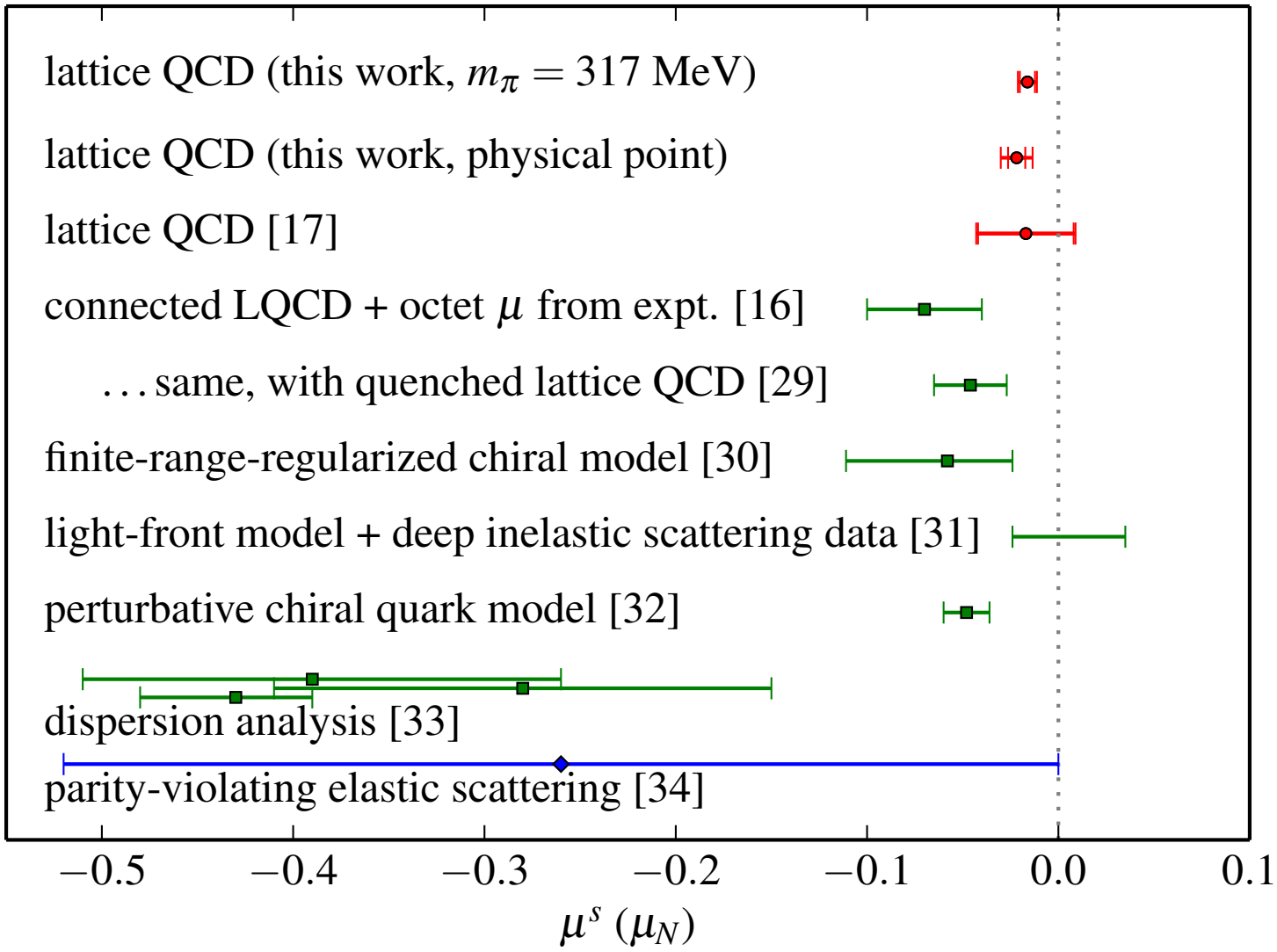

See also recent result at m_π^{phys}: $\mu^s = -0.073(17)(8)\,\mu_N$

R. S. Sufian, Y.-B. Yang *et al.* (χQCD Collaboration), 1606.07075

Strange magnetic moment

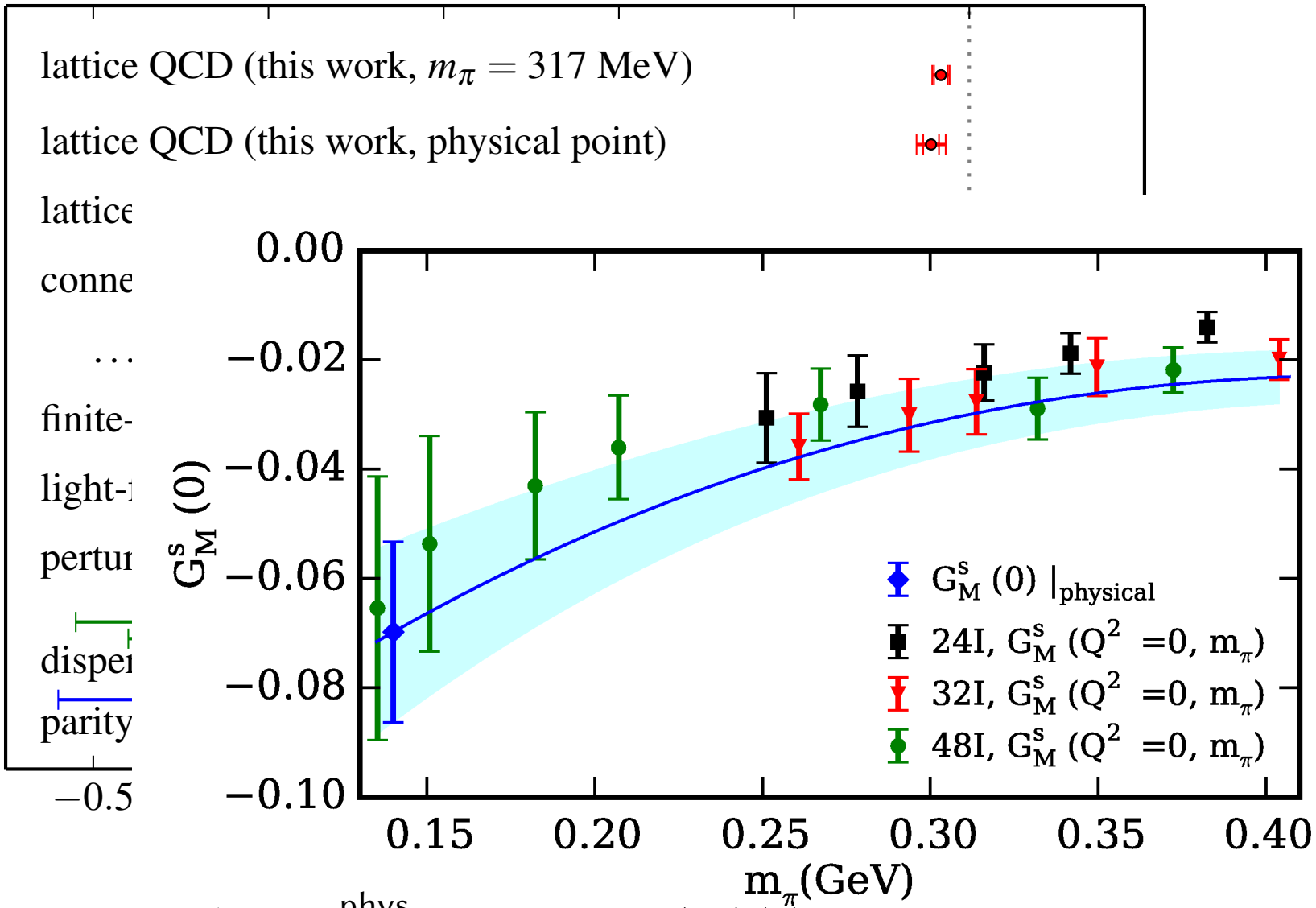

See also recent result at m_π^{phys}: $\mu^s = -0.073(17)(8)\,\mu_N$

R. S. Sufian, Y.-B. Yang *et al.* (χQCD Collaboration), 1606.07075

Forward-angle scattering experiments

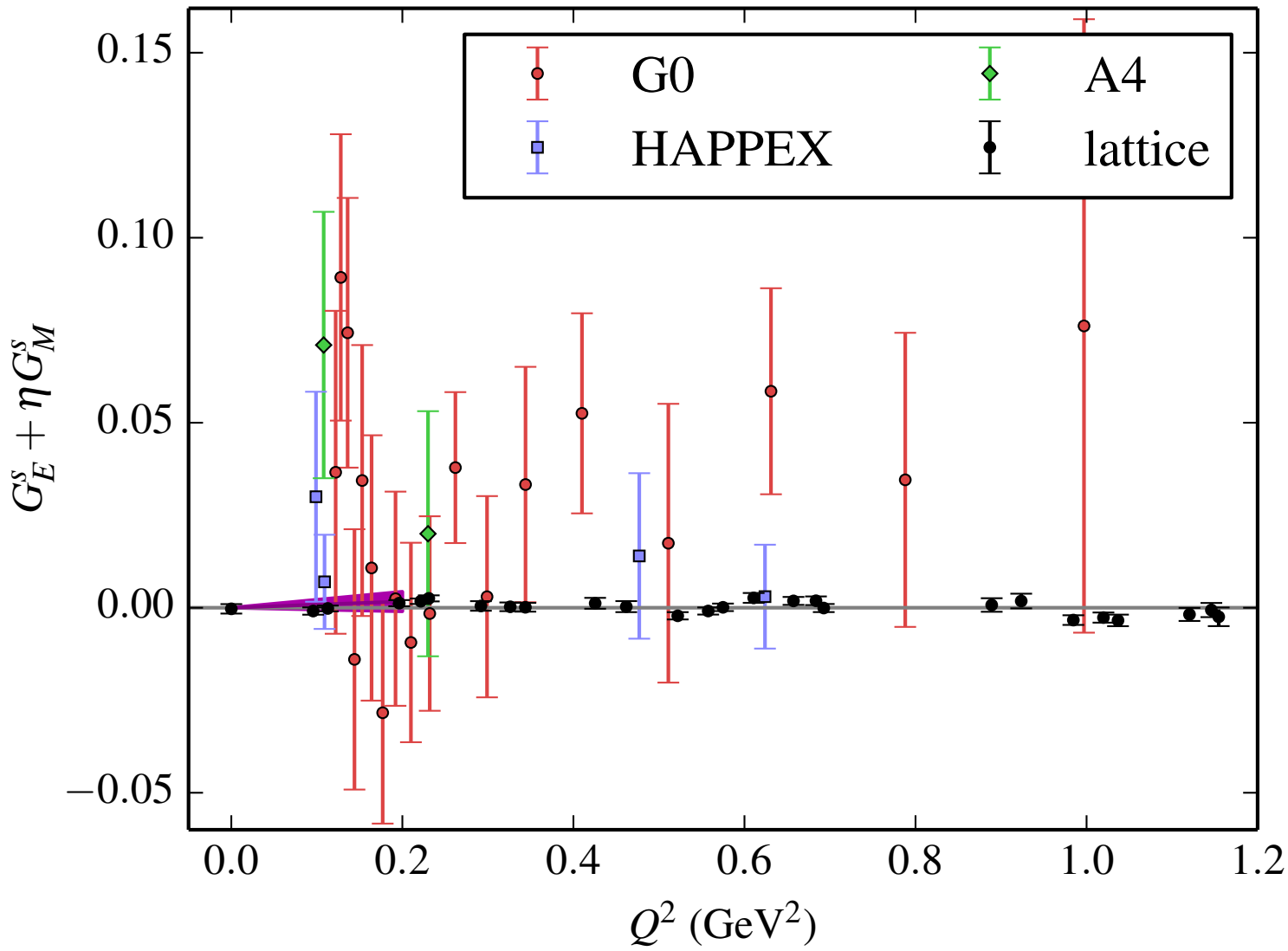

$\eta \approx AQ^2$, $A = 0.94$ GeV^{-2}

Combining lattice data with experiment

Recent work by A4 experiment at MAMI:

D. Balaguer Ríos *et al.*, Phys. Rev. D **94** (2016) 051101(R)

- New measurement of A_{PV}^{d} at $Q^2 = 0.224$ GeV^2, combined with two previous measurements of A_{PV}^{p} at forward and backward scattering angles.
- Axial and strange contributions parameterized by G_E^s, G_M^s, $G_A^{e,I=0}$, $G_A^{e,I=1}$, where the latter two are effective axial form factors including radiative corrections.
- $G_A^{e,I=0,1}$ have large theoretical uncertainty due to hadronic unknowns.
- Lattice QCD data were used to constrain G_E^s, allowing for the three other contributions to be determined from the three measurements.

Newer parity-violation experiments (Qweak, P2) are focusing on measuring the proton weak charge. Thus hadronic contributions are an unwanted systematic. Lattice calculations can help to confirm the smallness of strange form factor contributions.

Light and strange axial form factors

talk by JG (LHP Collaboration), Lattice 2016

Same $m_\pi = 317$ MeV dataset as for electromagnetic form factors.

Additional challenge: renormalization, which differs between flavour singlet and nonsinglet axial currents.

- Nonsinglet has zero anomalous dimension and is fairly straightforward.
- Singlet has nonzero anomalous dimension starting at $O(\alpha^2)$.
  - Perform matching and running to $\overline{\text{MS}}$ at $\mu = 2$ GeV.
  - Can reuse the previously-computed disconnected diagrams when evaluating the relevant observables for nonperturbative renormalization.

Singlet-nonsinglet difference causes mixing between A_μ^s and A_μ^{u+d} under renormalization.

Effect of mixing: G_A^s

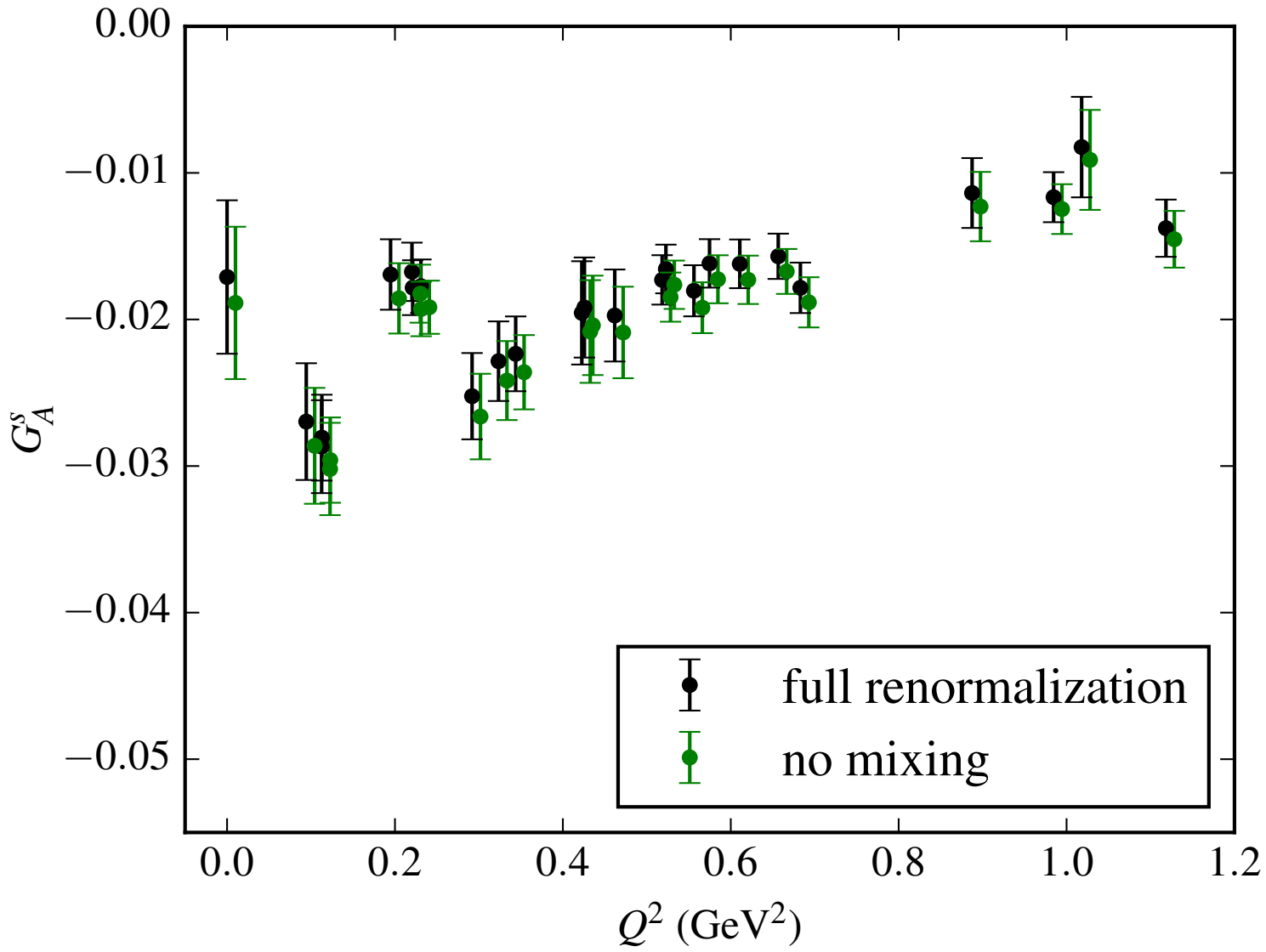

Largest effect: mixing of (large) G_A^{u+d} into (small) G_A^s.

G_A, disconnected

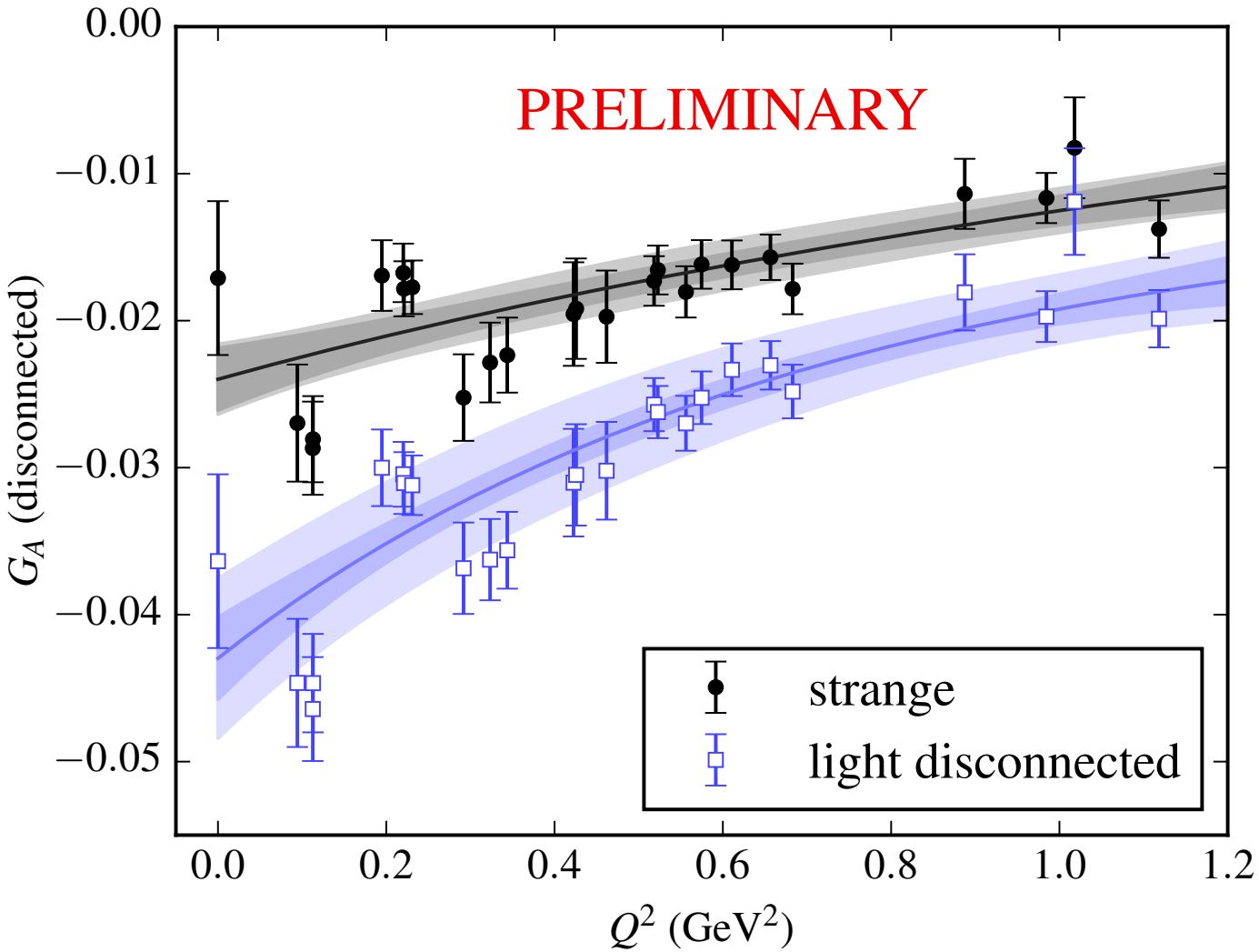

Fit (using z-expansion) produces more precise result at $Q^2 = 0$.

Systematic uncertainty for $G_A^{u,\text{disc}} = G_A^{d,\text{disc}}$ dominated by excited states.

Strange quark spin

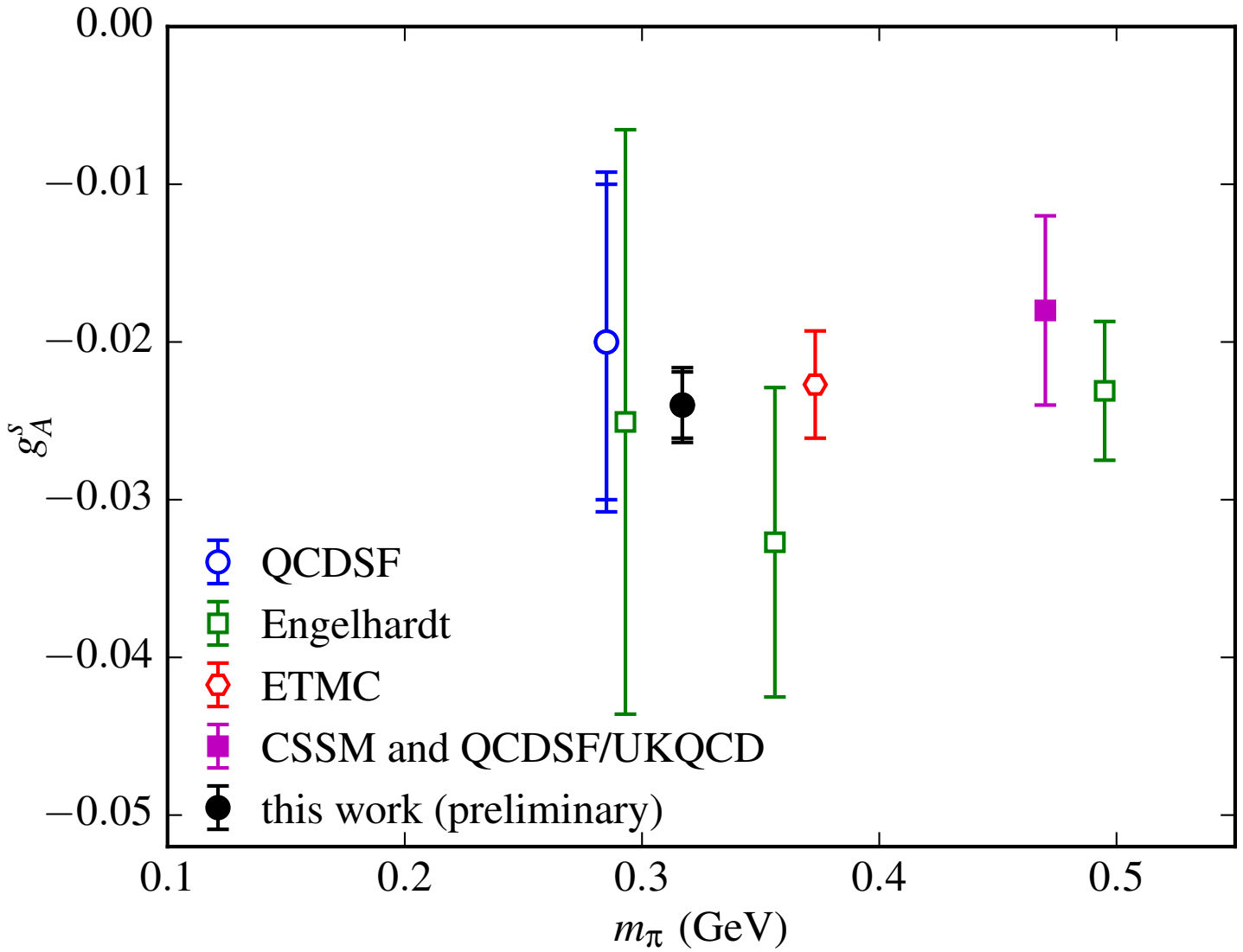

Comparison with published results.

G_P, isoscalar

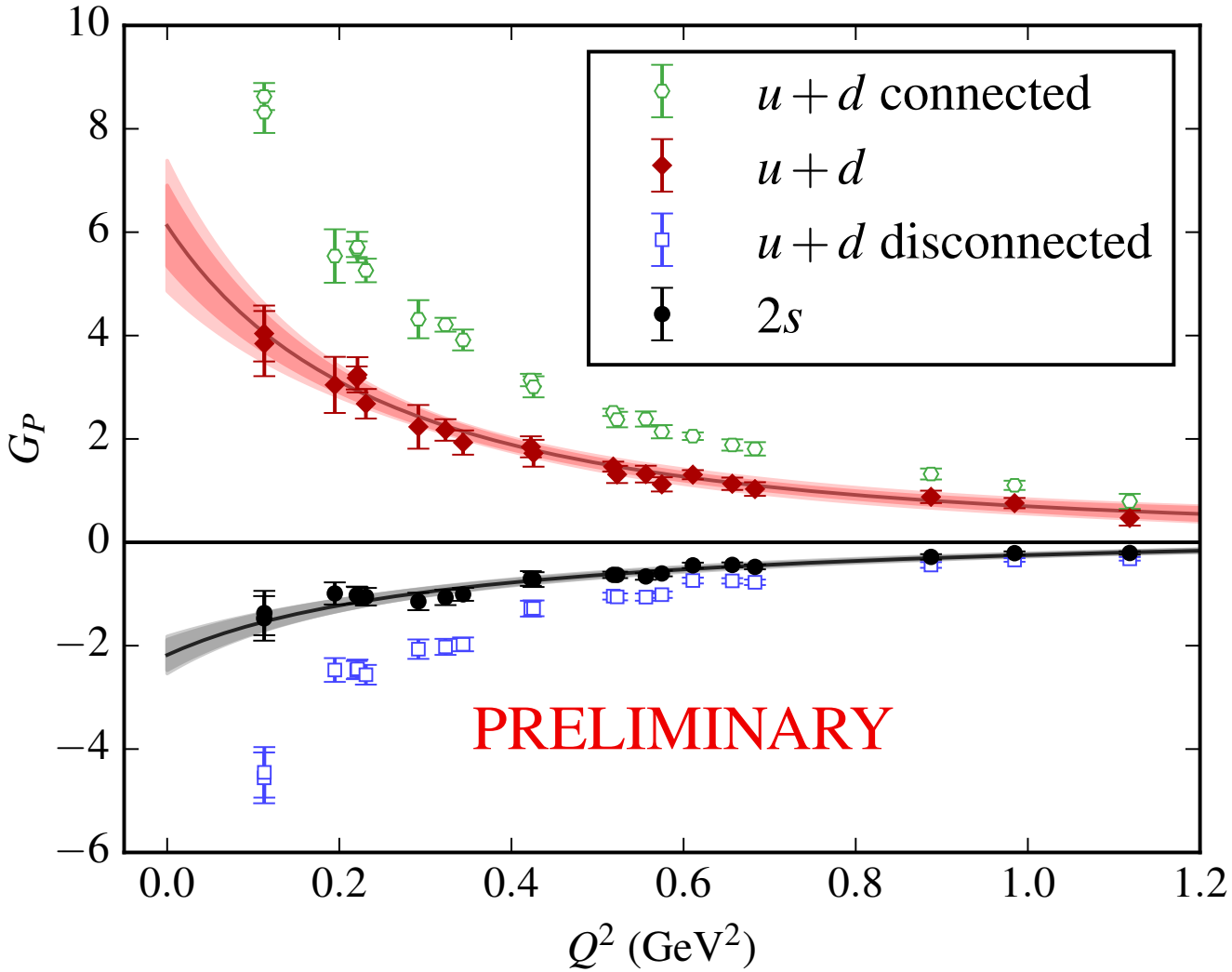

Connected $u + d$ seems to have a pion pole, cancelled by disconnected part.

Disconnected contributions are too large to neglect.

Conclusions and outlook

- High statistics and hierarchical probing methods are effective at producing a signal for the disconnected form factors.
- Strange quarks contribute a small amount to the proton radii and magnetic moment ($< 1\%$).
- Obtaining a clear nonzero strange-quark signal will be a significant challenge for future parity-violating elastic scattering experiments, especially at forward scattering angles.
- The difference between singlet and nonsinglet renormalization factors can be accounted for with reasonable errors. This is a small effect for axial currents.
- Preliminary value at $m_\pi = 317$ MeV: $g_A^s = -0.0240(21)(11)$.
- Significant cancellation occurs between connected and disconnected G_P, particularly at low Q^2. This may be caused by cancellation of a pion-pole contribution.
- Additional calculations, especially closer to physical quark masses, are needed to control systematic uncertainties.

Extrapolation to the physical point

We would like to extrapolate from unphysical quark masses using chiral perturbation theory (ChPT).
For u, d, and s quarks, and nucleons, we need $SU(3)$ heavy baryon ChPT.

- degrees of freedom: meson octet (π, K, η) and baryon octet (N, Σ, Λ, Ξ)
- known parameters: meson decay constant f, baryon axial couplings F, D

At leading one-loop order:

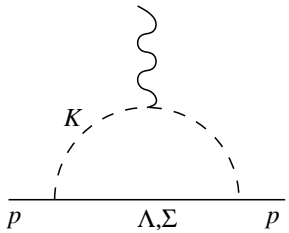

[M. Musolf, H. Ito, Phys. Rev. C **55** (1997) 3066
T. R. Hemmert *et al.*, Phys. Lett. B **437** (1998) 184
T. R. Hemmert *et al.*, Phys. Rev. C **60** (1999) 045501]

$$(r_E^2)^s = \frac{1}{16\pi^2 f^2}\left(c_1(\mu) + \frac{9+5c_{DF}}{3}\log\frac{m_K}{\mu}\right),$$

$$\mu^s = c_2 + \frac{m_p m_K}{24\pi f^2} c_{DF},$$

$$(r_M^2)^s = -\frac{m_p}{48\pi f^2 m_K} c_{DF},$$

where $c_1(\mu)$ and c_2 are unknown parameters, and $c_{DF} = 5D^2 - 6DF + 9F^2$.

Disconnected light-quark observables in ChPT

By themselves, the disconnected light-quark form factors are unphysical, but they can be understood in partially quenched QCD and partially quenched ChPT: $q \in \{u, d, s\} \to q \in \{u, d, s, l, \tilde{l}\}$.
At leading one-loop order, one can simply modify the mass of the strange quark in the loop, i.e., replace m_K with m_{loop}, where

$$m_{\text{loop}} = \begin{cases} m_K & \text{for strange quarks} \\ m_\pi & \text{for disconnected light quarks} \end{cases}$$

Thus with the leading one-loop formulas we can interpolate to the physical kaon mass.

Partially quenched ChPT at leading one-loop order

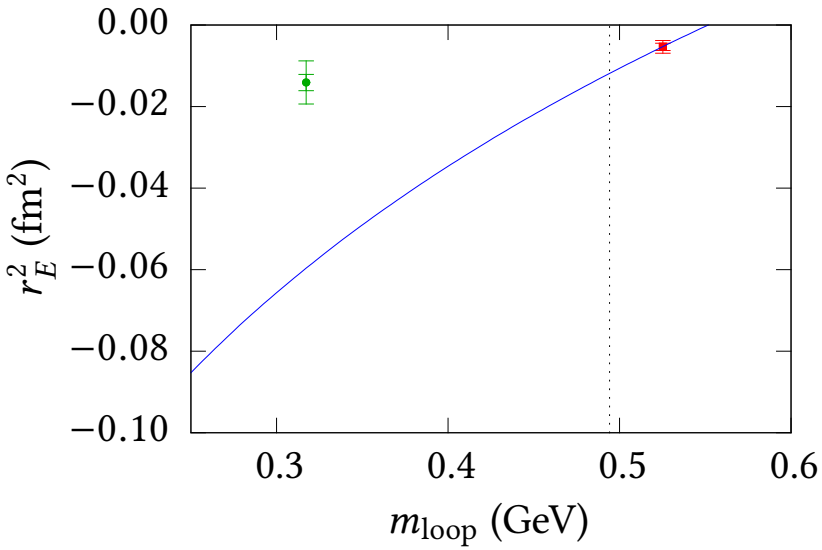

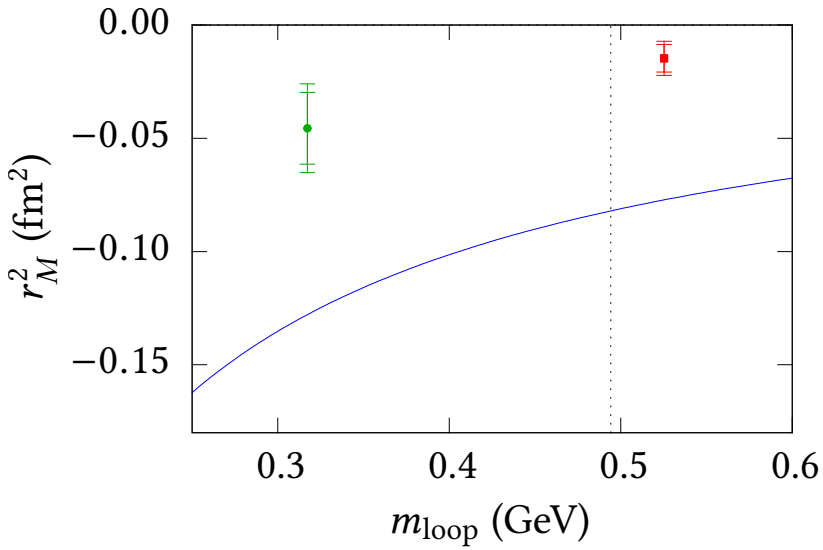

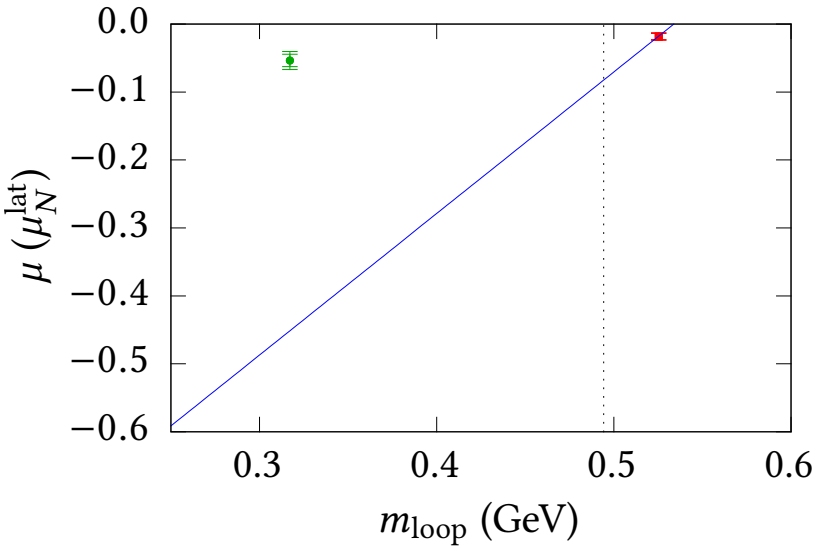

At this order, PQChPT poorly describes the data.
$\longrightarrow$ use simple linear interpolation in m_{loop}^2.

Strange magnetic moment and radii at physical point

Best estimate at physical quark masses: use linear interpolation in m^2_{loop}:

$$\begin{aligned}(r_E^2)^s &= -0.0067(10)(17)(15)\ \text{fm}^2,\\ (r_M^2)^s &= -0.018(6)(5)(5)\ \text{fm}^2,\\ \mu^s &= -0.022(4)(4)(6)\ \mu_N,\end{aligned}$$

where the uncertainties are

1. statistical
2. previously estimated systematics
3. physical-point extrapolation
   (= magnitude of shift from result at $m_\pi = 317$ MeV)